Nanoscale Measurements of Conducting Domains and Current−Voltage Characteristics of Chemically Deposited Polyaniline Films

Chun-Guey Wu* and Su-San Chang

Department of Chemistry, National Central University, Chung-Li, Taiwan 32054, Republic of China

Received: August 19, 2004; In Final Form: October 31, 2004

Spatial variations in electric conductivity and evolutions of band structures of polyaniline (PANI) films have been studied by use of a so-called current-sensing atomic force microscope (CS-AFM) or atomic force microscope current image tunneling spectroscopy (AFM-CITS). PANI films were deposited chemically onto indium−tin oxide− (ITO−) glass substrates, and their thickness and doping levels were controlled by polymerization and acid-doping conditions. The conducting uniformity of the PANI films depends on their doping level and thickness. Conducting domains were observed in fully doped PANI film, even when the bias voltage was reduced to as small as 30 mV. High current flowing regions gradually disappeared when conducting PANI films were partially dedoped. The point-contact current−voltage ($I-V$) characteristics of conducting tip-polymer/ITO systems were investigated on PANI films with different thickness and degree of doping. Various types of $I-V$ curves representing metallic, semiconducting, and insulating states were obtained depending on the aggregation of polymer chains and doping level of the polymer film. The band gap energies (estimated from the $I-V$ or $dI/dV-V$ curves) of emeraldine base (EB) (undoped polyaniline) films are all higher than 3.8 eV, and a wide distribution of the band gap energies (0−1.1 eV and 0.75−1.8 eV for fully and partially doped PANI thin films, respectively) was found in a single polymer film.

Introduction

Recently, nanoscale electronic devices using conducting polymers have attracted much attention for the construction of fast, inexpensive, and dimensionally appropriate devices.[1] In most of these applications, both their bulk and interfacial electrical properties are decisive; in other words, the dopant ion distribution in the conducting polymer films and electron transfer through the interface are key factors in determining the performances of the devices. Therefore, it would be very important to have a good understanding of their interfacial electronic states, their electron transport properties, and how homogeneous they are in the nanoscale, if one wants to use their electrical properties in nanoscale devices. Moreover, it is imperative (but difficult) to reproducibly and accurately measure and evaluate the electrical properties of the materials in nanoscale.

Scanning tunneling microscopy (STM) has been widely used to measure the electrical characteristics of single molecules and their assemblies that are of interest to molecular electronics.[2] However, use of the STM technique for this purpose is limited to conducting materials or very thin nonconducting materials due to the restriction of the typical tunneling distances (1−10 nm). The STM results also include the vacuum gap between the tip and molecules probed, which can cause complexity and ambiguity in the interpretation of intrinsic properties of molecules. There also have been a few reports on the electronic states of conducting polymer films studied by the Kelvin probe method.[3] Nevertheless, this method can be used only for mapping the surface potential, not for direct quantitative studies. On the other hand, atomic force microscopy with a conducting tip (CS-AFM) has found its applications in many areas because it allows an easy contact to be made with various substances including organic materials.[4] Furthermore, the contact can be made between the conducting tip and the substrate with a certain confidence by maintaining a prescribed load force. Topographical and current images could be obtained simultaneously for various systems, which provide otherwise impossible information on the distribution of conducting islands surrounded by insulating areas. Furthermore, the current−voltage ($I-V$) traces can provide the relations between structural features and electrical properties of the materials on the nanometer scale.[5]

Polyaniline (PANI) is a prominent intrinsically conducting polymer, due to its unique combination of high conductivity, easy preparation, and technologically usable products such as films and fibers. There are a large amount of scientific works dealing mainly with its charge carriers and the way in which the carriers move in polymer chains and polymer films.[6] It was also shown that localized variations in the thickness, stoichiometry, defects, or even substrates[7] of the PANI films are also factors believed to influence the localized conductivity. We had succeeded in preparing of highly conductive polyaniline films via in situ polymerization/deposition of aniline on modified indium−tin oxide (ITO) substrates.[8] The preliminary results on the atomic force microscope current image tunneling spectroscopy (AFM-CITS) and transmission electron microscopy (TEM) studies of the as-prepared polyaniline film have been reported.[9] In the present report, AFM-CITS is used to image the heterogeneous electronic conductivity of PANI films with various thicknesses and degree of doping on ITO substrates. The AFM-CITS investigation reported herein is the attempt to directly quantify the heterogeneous electronic structure of PANI films at various doping levels. In this paper, we demonstrate that AFM-CITS could be applied to reveal both the spatial conductivity by mapping current images and the band gap by

* Corresponding author: tel 011886-3-422-7151, ext 5903; fax 011886-3-422-7664; e-mail t610002@cc.ncu.edu.tw.

10.1021/jp046259b CCC: $30.25
Published on Web 12/15/2004

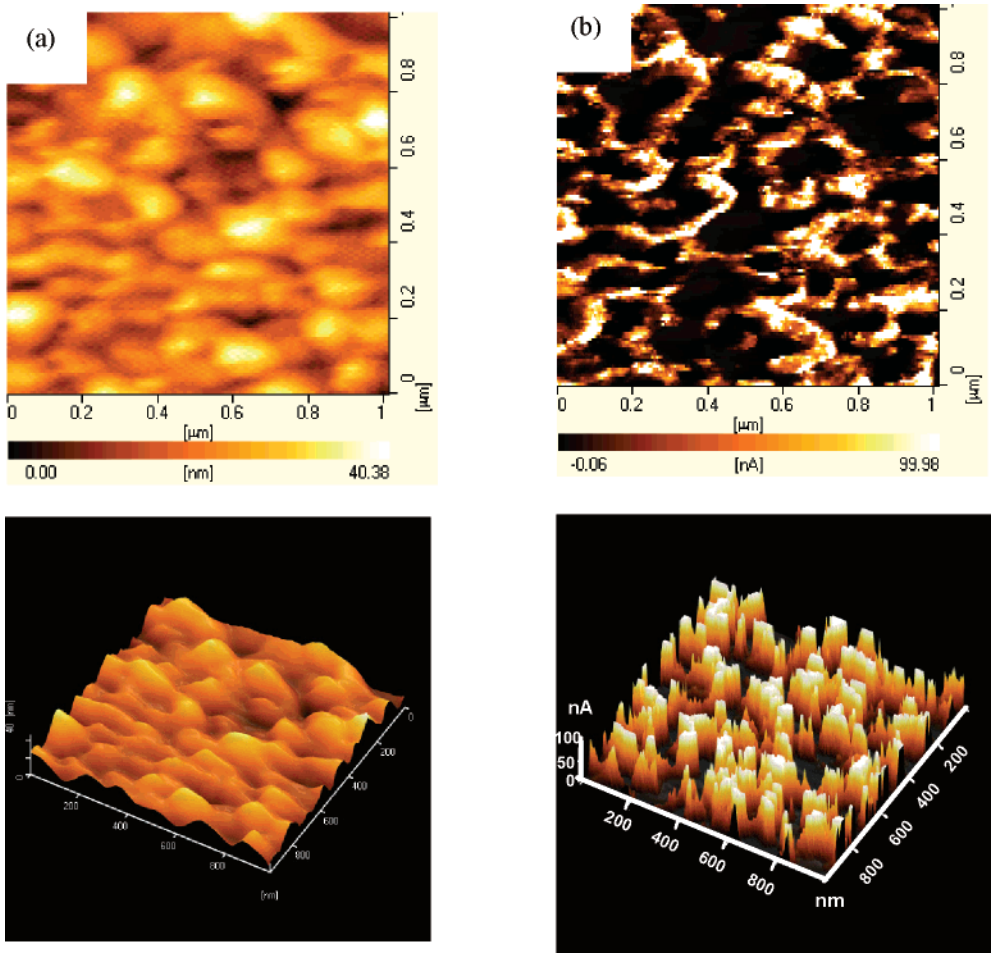

Figure 1. (a) Topography and (b) CITS images of fully doped PANI film (bias voltage 0.5 V; film thickness 130 nm). Top, two-dimensional images; bottom, three-dimensional images.

measuring $I-V$ curves as a function of the applied voltage for the in situ chemically deposited polyaniline films.

Experimental Section

Chemicals. Water was purified on a Milli-Q (Millipore Corp., Bedford, MA) purification system with a resistivity of 18 MΩ cm. ITO substrate (Merck Display Technologies Ltd. with ITO thickness of 100 nm and surface resistance of ∼20 Ω/) was cut into 20 × 20 mm. Aniline (Acros, ACS grade) was used after distillation over calcium hydride powder and stored in the dark under a nitrogen atmosphere. HCl (aq), NH_4OH (aq), and $(NH_4)_2S_2O_8$ were obtained from commercial resources and used without further treatment.

Preparation of PANI Films. Polyaniline films on ITO substrates were prepared as reported in the literature.[8] Prior to analysis, each sample was first dipped in 0.1 M NH_4OH (aq) [to ensure that it is fully dedoped to emeraldine base (EB)] for 5 min, washed with distilled water, and dried under a stream of N_2 gas. The film thickness was determined to be 100∼300 nm by a Veeco Instruments Dektak3 surface profiler and the absorption intensity at 600 nm. The calibration curve of absorption intensity vs film thickness was obtained by measuring the absorbance at 600 nm as well as the thickness (SEM images of the film cross-section) of the PANI films. The degree of doping of PANI films was controlled by dipping the EB films into the acidic solution of different concentrations for various periods of time. UV/Visible spectra (taken from the Cary 5E photospectroscope) were used to monitor the doping level of PANI films.

AFM-CITS Studies. Samples for AFM-CITS studies were mounted, via silver paste, to the AFM sample holder. Before imaging of the PANI surfaces, the surface was purged by N_2 gas to minimize the effects of moisture. The contact-mode AFM with a current-sensing module (SPA400, Seiko Inc., Japan), also called a current image tunneling microscope,[10] was used to simultaneously obtain topographical and current images. Topography images were recorded in the height mode. In height mode, the changes in the *z*-piezo position required to maintain a constant cantilever deflection caused by variations in the surface topography are recorded. The gold-coated Si cantilevers (spring constant 0.11 N/m) were purchased from Nanosensor Co., Germany. The load force was maintained at ∼0 N to avoid damage to the tip and the sample. A bias voltage between the substrate (ITO) and conducting cantilever (which is grounded) for CITS images were scanned from −1.6 to +1.6 V. The best bias voltage to show the conducting homogeneity of polymer film varied from sample to sample, depending on the conductivity and conducting homogeneity of polymer films. The electrical conductivity of each tip was verified before and after each set of experiments by measuring the tip current that flowed when the probe was placed in contact with a metal surface under an applied bias. The data were discarded whenever the images or the tip conductivities were different before, during, or after electrical measurements.

Results and Discussion

Synthesis of PANI Films with Various Thicknesses and Degrees of Doping. PANI films used in this study were

prepared by in situ polymerization/deposition of aniline on ITO in HCl (aq) solution at 0 °C. The thickness (130∼300 nm) of PANI films was controlled by deposition time as well as the concentration of aniline in acidic aqueous solution. The as-prepared PANI film is an HCl-doped emeraldine salt (ES). To measure the thickness (by use of UV/vis spectrum) and exchange dopants, the as-prepared films were dipped in 0.01 M NH_4OH (aq) for 2 min to convert ES to undoped emeraldine base (EB). The thickness of the EB film was measured with a surface profile meter and further confirmed with the SEM images as described in the Experimental Section. To control the doping level, EB film was dipped in 0.01 M HCl (aq) for a certain period of time and the UV/vis spectra were taken. The degree of doping of PANI films was calculated from

$$D\,(\%) = \frac{{}^{S}\lambda_{max} - {}^{EB}\lambda_{max}}{{}^{ES}\lambda_{max} - {}^{EB}\lambda_{max}} \times 100 \qquad (1)$$

where D is the degree of doping,

${}^{S}\lambda_{max}$ is the absorption maximum of the sample,

${}^{ES}\lambda_{max}$ is the absorption maximum of the fully doped polyaniline, and

${}^{EB}\lambda_{max}$ is the absorption maximum of the undoped polyaniline.

Local Conductivity of PANI Films. Figure 1 shows typical topography (a) and current (b) images obtained simultaneously for an identical part of the surface of a fully doped PANI film. The globular-shaped structure in the topographical image is typical for film thickness below 1 μm, although the size and shape are slightly different depending on the doping level and thickness. The conductivity images in Figure 1, recorded by applying a bias voltage of 500 mV, demonstrate that electron conduction across the PANI film is heterogeneous, with localized regions of high conductivity on length scales ranging from 10 nm × 10 nm to 20 nm × 150 nm dispersed within an insulating region. The contrast observed in the current images is due to the differences in the conductivity of the PANI film, and the conductivity is not totally dependent on the topography. The shapes and sizes of the grains observed in the topography images shown in Figure 1a are consistent with the scanning electron microscopic (SEM) images. Both AFM and SEM indicate that the grain size is on the order of 50∼100 nm.

The current upper limit used for our measurements, i.e., 100 nA, is the maximum value our current amplifier can handle. Therefore, we could not distinguish the conductivity between various points on the surface with currents higher than 100 nA. We thus needed to use smaller bias voltages and examined the polymer film under the same experimental conditions to see the conductivity homogeneity in high-conducting (current higher than 100 nA) areas. Figure 2 showed the current images of a fully doped polyaniline film at two different bias voltages. The topography images (not shown here) are practically identical at different applied bias voltages; however, the current images are quite different. The highest current is 58 nA at the applied bias voltage of 100 mV; nevertheless, saturated current (>100 nA) was observed in several areas when the bias voltage is 250 mV. As can be seen in Figure 2, distinguished conducting domains were revealed only at certain bias voltages. Therefore, the following current images were displayed at different bias voltage to display clearly the conducting homogeneity. Fluctuations in the conductivity that occur over length scales as small as 10 nm are readily apparent in the higher magnification image, in which the topography image is very vague.

AFM-CITS Images of PANI Films with Different Doping Levels. Large fluctuations in film conductivity are observed not only on fully doped PANI films but also on the partially doped films. For example, Figure 3 shows a high-resolution topography and current images of polyaniline films with various degree of doping, obtained at a bias voltage of 500 mV. The height-mode image of the region of interest shows that the surface topography is essentially independent of doping level. The corresponding current image of the same region, however, reveals a different conductivity. Higher conductivity (higher tunneling current) was observed in polyaniline with higher degree of doping. Thus, the highly conductive region clearly suggests that the area is highly doped. Although our CITS measurements do not provide direct assessment of the chemical identity of the more conductive surface regions, it appears highly likely that these regions correspond to the fully doped PANI chains previously identified by spectroscopic methods. Conducting islands surrounded by insulating sea were observed in fully doped PANI film as proposed before.[6d] The CITS image of emeraldine base (undoped polyaniline) showed no current flow at bias voltage less than 4.0 eV. As the doping level increased, the size of conducting islands increased and at the same time the tunneling current also increased significantly. There is no observable preferential doping or dedoping site as was observed by Lee

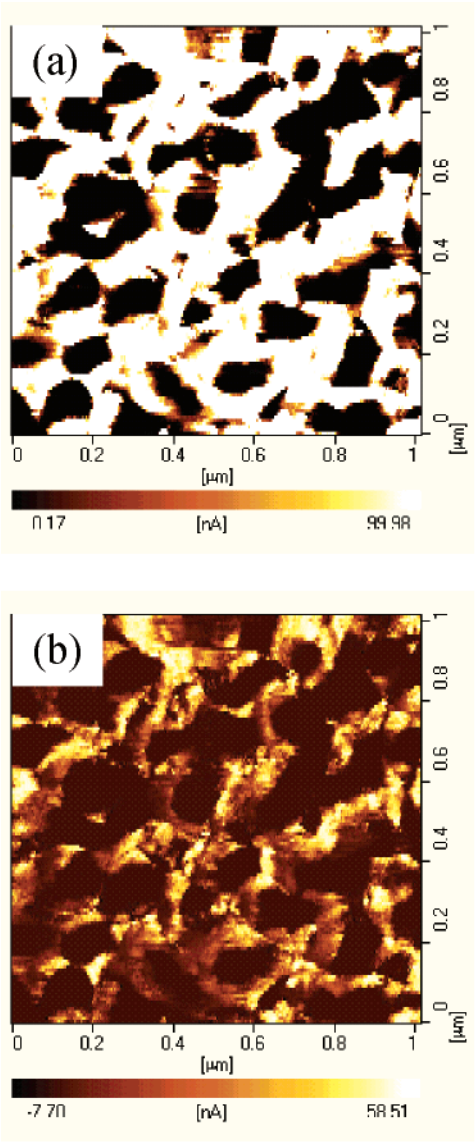

Figure 2. CITS images of fully doped PANI film (185 nm) at applied bias voltage of (a) 0.25 V and (b) 0.1 V.

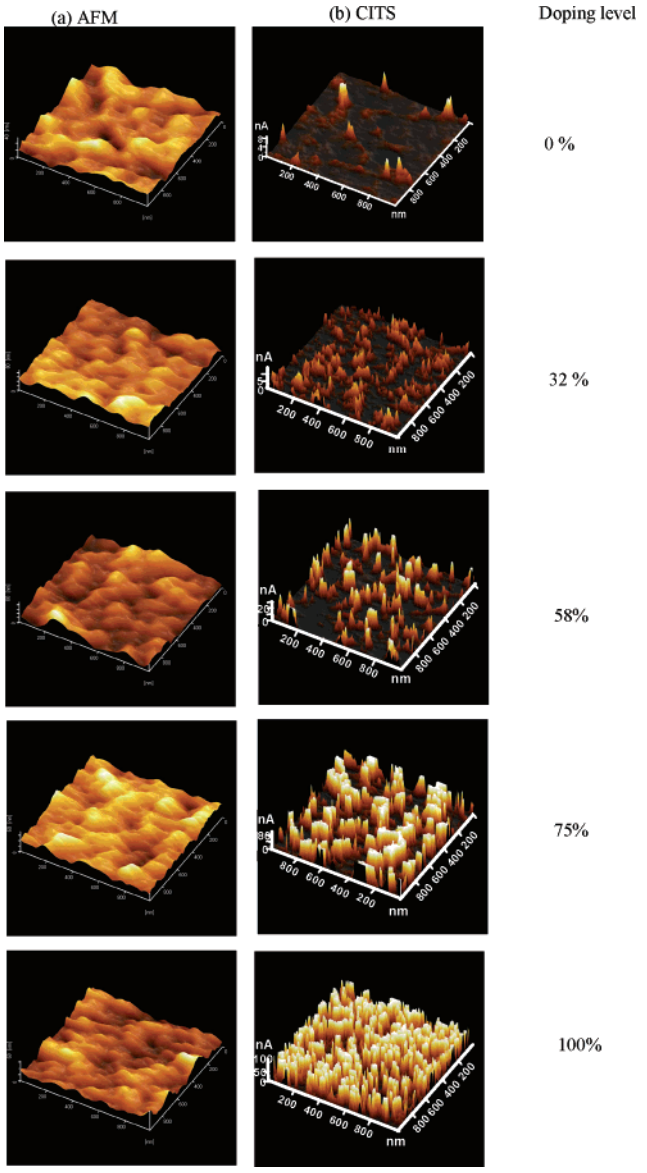

Figure 3. (a) AFM and (b) CITS images of PANI films at various doping levels (bias voltage is 4.0 V for EB and 0.5 V for the others).

and Park,[11] who found that the top of the globules in electrochemically prepared polypyrrole film is preferentially reduced.

It is seen fairly clearly from the current image shown in Figure 3b that the local conductivity of PANI film is not homogeneous at all doping levels. For example, the highest conducting domain of the PANI film with 58% doping can be as large as 20 nm × 200 nm. Areas of no current (very low conductivity) are detected and larger domain sizes of middle conductivity are also observed. Fluctuations in film conductivity were also observed where height changes in the topography images are not severe, suggesting that the conductivity within the grain is also inhomogeneous. Therefore, the contrast observed in the conductivity images is due to the differences in the conductivity of the polymer film with no direct relation to the morphology. The conducting inhomogeneity of partially doped PANI film is perhaps due to the fact that some regions are more doped and, thus, more conductive than other regions. When a spot is more doped, it may accept electrons more easily than the other locations due to a larger conductivity at the spot. When PANI film was subjected to doping, the regions where high currents flow were spread over the surface and the magnitudes of currents

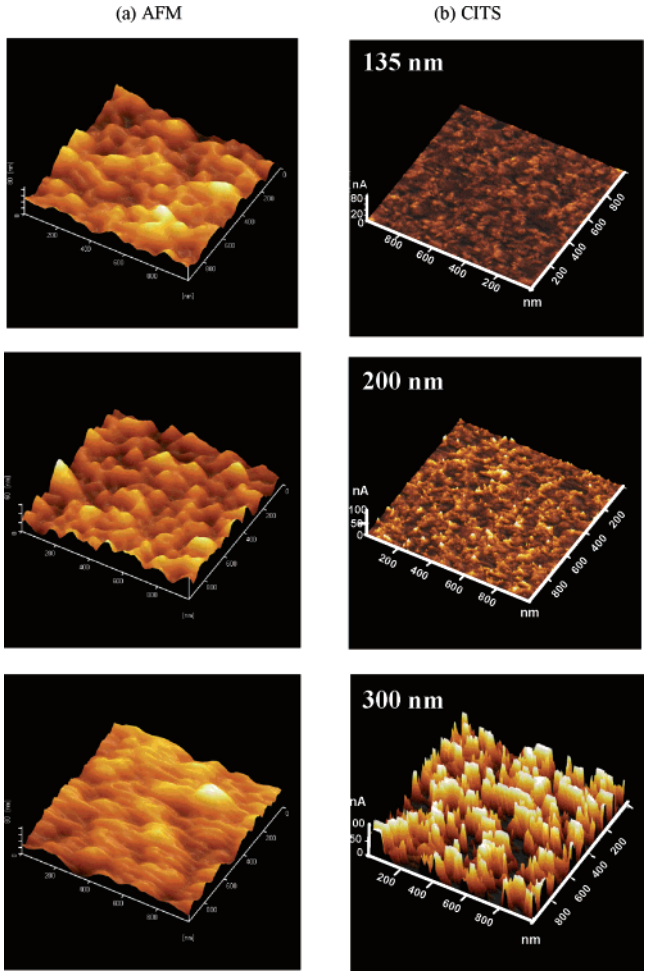

Figure 4. (a) AFM and (b) CITS images of fully doped PANI films at various thicknesses (bias voltage 0.01 V).

were also increased, as shown in Figure 3. Nevertheless, even when the polymer film was fully doped, there still were some spots that showed low conductivity. Those low conducting spots can be regarded as defects [cannot be fully doped by HCl (aq)] of the polyaniline film. The results described here indicate the fully doped and partially doped films are fairly inhomogeneous in electrical characteristics.

AFM-CITS Images of Fully Doped PANI Film in Various Thicknesses. It seems that the doping level will affect the conducting homogeneity of PANI films. It is interesting to know the effect of film thickness on the conductivity and conducting homogeneity of the fully doped PANI films. It had been reported[12] that the STM images of polypyrrole and polythiophene conducting polymers revealed highly ordered structures near surfaces that transform to amorphous structures with increasing film thickness. What kind of structure will be observed in polyaniline films? The topographical and current images of PANI film with three different thicknesses are displayed in Figures 4. The topographies of fully doped PANI film at various thicknesses (Figure 4a) were not totally similar to each other. The globular morphology was observed at film thickness less than 200 nm. When the thickness of PANI film is higher than 300 nm, the surface of the film becomes rather smooth. It was also found that the change in thickness led to a variation of the current images. One can see from Figure 4b that the current is small (the currents are significantly lower than the limiting value for the instrument) and therefore seems homogeneous at thin PANI film. Nevertheless, in thicker films, apparent conducting islands, at which high currents flow, are

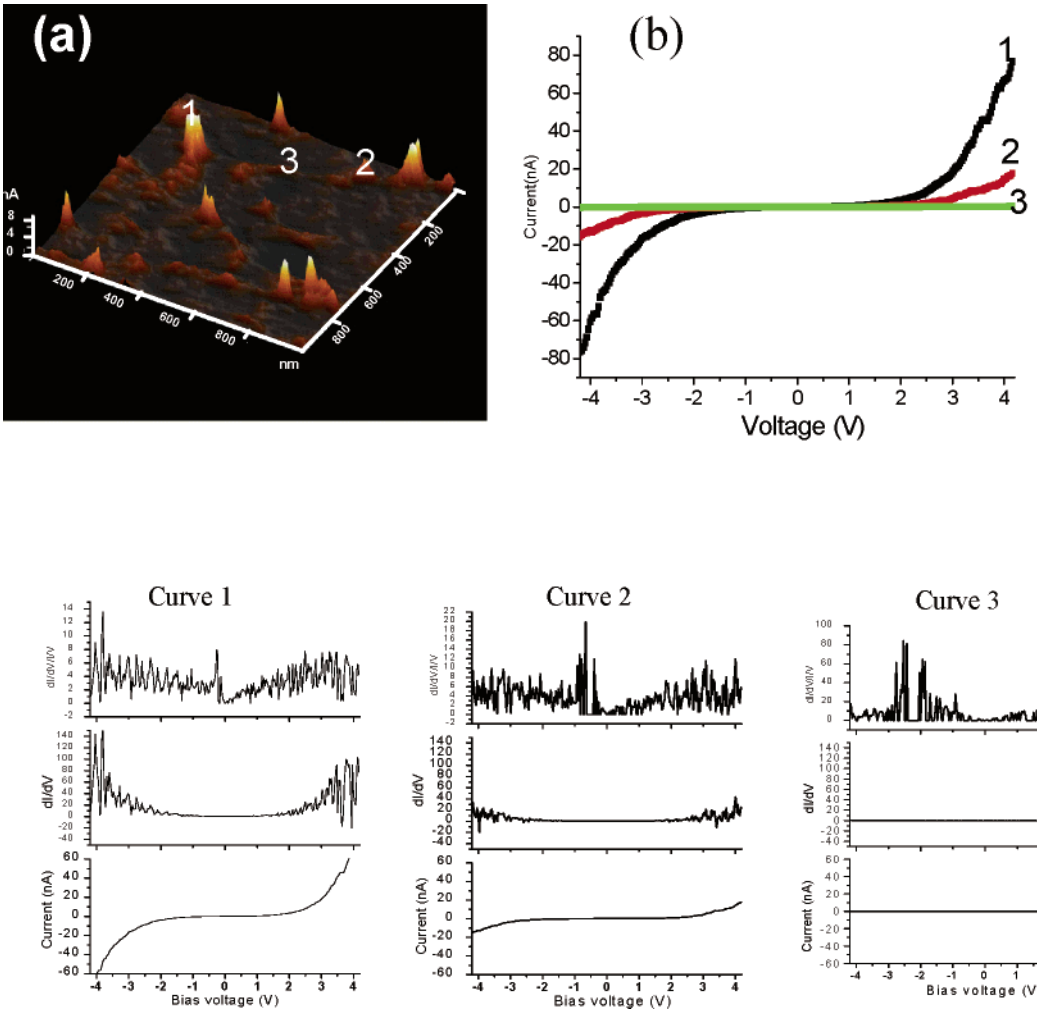

Figure 5. (a) CITS image, (b) $I-V$ curve, and (c) differential conductance (dI/dV vs V) of EB film (200 nm thick).

TABLE 1: AFM and CITS Data of Doped Polyaniline Films[a]

film thickness (nm)	135	200	300
RMS-S[b] (nm)	11.2	8.4	8.9
RMS-I[c] (nA)	1.1	2.8	26.6
P − V[d]	10.5	22.7	100
I_a[e] (nA)	0.67	3.95	f
I_{max} (nA)	10.5	22.9	>100

[a] Applied bias, 0.01 V; scan area, 1000 nm × 1000 nm. [b] Root mean square of the surface roughness. [c] Root mean square of the current inhomogeneity. [d] Difference between highest current and lowest current. [e] Average current. [f] The current of some areas is higher than 100 nA (the limit of the instrument), therefore, the average current cannot be calculated accurately.

isolated by large lower conducting regions. The conductive islands did not necessarily correspond to the top of the globules. The high current flowing regions are fairly homogeneously dispersed and some currents are higher than the limiting value (100 nA) of the system we used. Furthermore, for thick (300 nm) films, more high conducting area with the current higher than 100 nA at the applied bias voltage of 0.003 V were detected. These observations are attributed to the aggregation of the polyaniline chains in polymer films. The polymer films studied in this article were prepared by in situ polymerization/deposition of aniline on ITO substrates. The thickness of the polymer film was controlled by the deposition time, although the mechanisms of the polymerization of monomers and the deposition of polymer chains on ITO substrate are not totally understood. However, the topographic images showed that rather smooth morphology was observed in thicker films. This result suggested that polymer chains in thick films were packed comparatively closer and more ordered. The aggregation and arrangement of polyaniline chains are two important factors that determine the conductivity and electric behaviors of the PANI films. The thickness-dependent current patterns and magnitudes shown here would explain why different conductivities and electrical properties were found in bulk conducting polymer films prepared under different experimental conditions. The AFM and CITS data for fully doped polyaniline films with various thicknesses are summarized in Table 1.

Evolution of the Band Gap of PANI Film Based on the Current Images under Various Bias Voltages. In efforts to assess the conductivities and band gap energies of these PANI films more quantitatively depending on the doping levels and thickness, we measured the current−voltage ($I-V$) curves at some selected spots. The electrical characteristics of the conducting and nonconducting regions were investigated by recording the tip current (I) as a function of the bias voltage (V). To obtain the $I-V$ curve, I is continuously measured as function of V, which is linearly scanned from +4.2 to −4.2 V for undoped polyaniline film and from +1.6 to −1.6 V for fully and partially doped polyaniline film at steps of 32.8 and 12.5 mV, respectively. The conductivity of EB film (200 nm thick) is very low; therefore, no current flow was detected at the bias voltage smaller than 4.0 V. The CITS images were taken at the bias voltage of 4.0, as displayed in Figure 5a. Inspection of the three $I-V$ curves at different areas of EB film reveals that the

current flow at all regions is very small (<5 nA at 4.0 V for highest conducting area). This trace amount of current may come from the low conducting EB film (since EB was regarded as a high band-gap semiconductor) or instrument. Therefore, it is hard to estimate the conductivity of EB film from the $I-V$ curves. Interestingly, the band gap energy (E_g), obtained from dI/dV vs V of the highest conducting area, was ca. 3.8 eV, consisted with the $\pi-\pi^*$ transition energy of EB film obtained from the λ_{max} of the UV/vis absorption spectrum (not shown here) and theoretic calculation.[14] The E_g of low conducting areas are all greater than 4.0 eV (see Figure 5c).

Upon doping of the EB film, depending on the doping level, not only the band gaps but also the population of the dopants would be different, leading to different conductivities. Therefore, we expect the electric characteristics of partially doped PANI film may differ from those of fully doped PANI film. Figure 6 showed the CITS image and $I-V$ characteristics of a partially doped polyaniline film. The results showed that the conductivity of partially doped polyaniline film was inhomogeneous and various $I-V$ curves can be obtained when the point-contact measurements are made over the film. The conductivity image in Figure 6a, recorded by applying a bias voltage of 0.1 V (tip vs substrate), demonstrated that electron conduction across the polymer film is inhomogeneous, with localized regions of high conductivity on length scales ranging from 10 to 30 nm dispersed within low conducting regions. A more likely possibility of the conducting inhomogeneity of polyaniline film comes from the differences in the degree of doping and the arrangement of polyaniline chains. In other words, the polyaniline chains are nonstoichiometric and aggregated divergently as a consequence of the difference in the film preparation conditions in the partially doped film. Furthermore, the structure defects of the polyaniline chains also affect the degree of doping and therefore the conductivity. So far, we did not have a good way to prove which could be the major factors causing the conducting inhomogeneity of polyaniline film.

The $I-V$ curves taken from some selected points were shown in Figure 6b. These curves represent the typical $I-V$ traces obtained frequently and reproducibly depending on doping levels of the films. All $I-V$ curves exhibited semiconductorlike characteristics. The conductivity, σ_p, of the doped PANI film within each region, in which the current is not limited by the instrument, was estimated from the $I-V$ curves by use of

$$\sigma = d/(A_t R)^{7c} \qquad (2)$$

where

σ is conductivity; d is film thickness,

A_t is the area of the C-AFM probe in contact with the surface (A_t was computed as πr^2, with the assumption that the contact radius between tip and sample is 50 nm); and

R is the resistance of the sample, estimated from the inverse slope of the $I-V$ curve. When the $I-V$ curve is not linear, the slope of the curve was estimated from the linear fit of the curve.

By use of this approximate approach, the conductivity of all conductive regions shown in Figure 6a were estimated to be 5.3×10^{-3}, 1.2×10^{-3}, and 6.0×10^{-4} S/cm respectively, 10 times difference in conductivity. The conductivity data also indicated that the dopants did not distribute homogeneously in every polymer chain in partially doped PANI film. During the first stage of doping, the easily doped area will be doped first, and then doping will gradually expand randomly to other areas. In a single polymer film, some areas may not be able to be doped fully under any experimental conditions. Moreover, it seems that a high degree of doping created more high conducting sites but not larger conducting domains, as revealed in Figure 3. The first-doped area is the area where the polymer chains aligned orderly and without structural defect. Since PANI film with highly ordered, perfect structure polymer chains in macroscale has not been synthesized yet, real macroscale high conducting PANI film has not materialized.

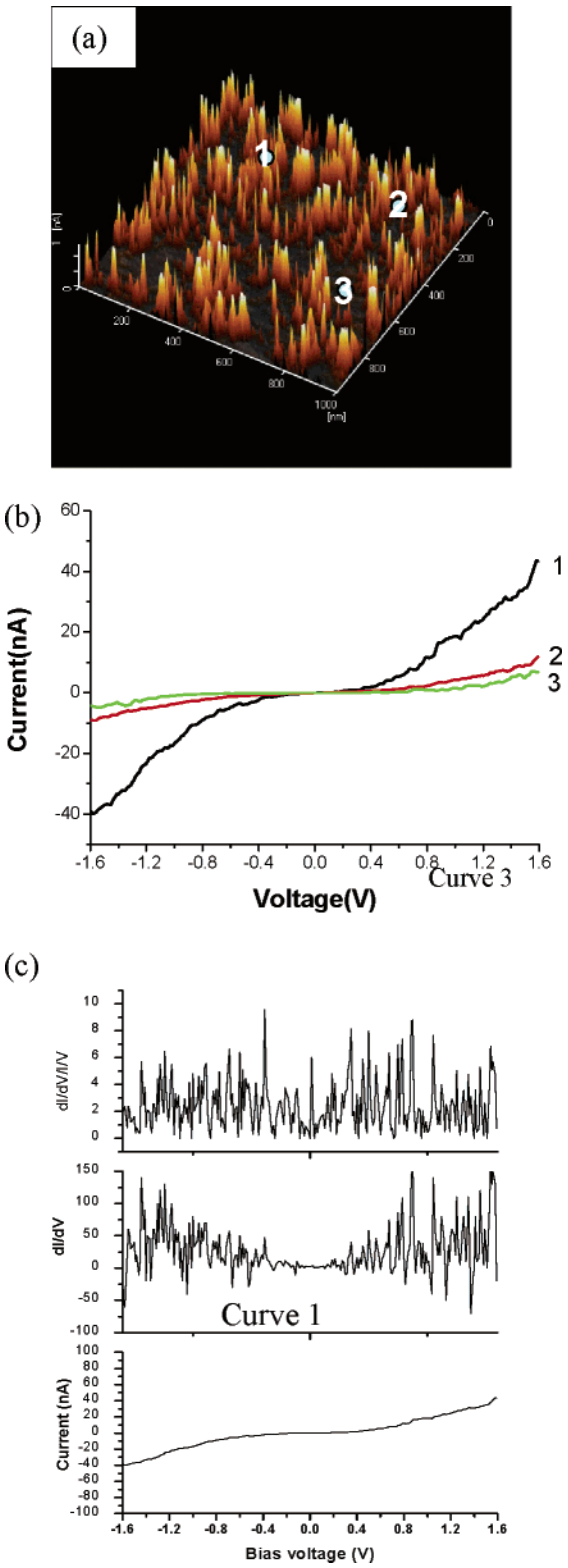

Figure 6. (a) CITS image, (b) $I-V$ curve, and (c) differential conductance (dI/dV vs V) of partially doped PANI film (200 nm thick).

To obtain the band gap of a partially doped PANI film, the $I-V$ curves were examined carefully, because all $I-V$ curves showed a semiconducting characteristic with various band gap

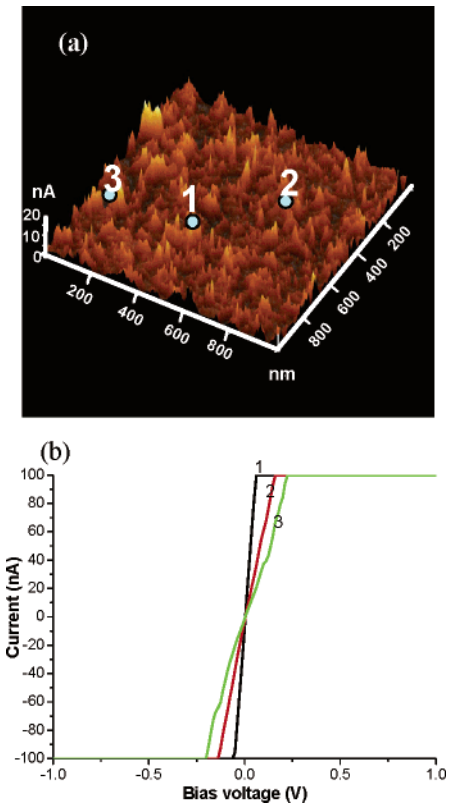

Figure 7. (a) CITS image and (b) $I-V$ curve of fully doped PANI film (200 nm thick).

energies. The $I-V$ curves shown in Figure 6b are not symmetrical with respect to 0 V. This is a behavior generally observed from a typical semiconductor−metal junction. A typical semiconductor−metal junction shows different current responses for forward and reverse biases.[15] Thus, partially doped PANI film examined here showed a typical characteristic of semiconductors. The band gaps estimated from the distances between the dI/dV peaks[13] not shown here are 0.75, 1.45, and 1.8 eV for curves 1, 2, and 3, respectively. However, as can be seen, the band gap (for example, higher conducting area, curve 1) may be estimated to be 0.75∼2.0 eV, depending on which peak signals are taken for band gap estimation from various band edges shown as peaks in the derivative signals (Figure 6c). There are a number of band edges, probably because various states generated during the doping process are located within the band gap due to the introduction of polarons and bipolarons, which also widens the band gap. The band gap widening is well-known for conducting polymers upon electrochemical doping.[16] There were some small peaks in Figure 6c; whether there are actual DOS features or background noise signals remain unresolved. The semiconducting properties derived from doped conjugated polymers could be different from those of true (inorganic) semiconductors. Conducting polymers become metal-like conductors when heavily doped[17] because interstate bands arising from bipolarons make the band gap small enough to make the holes move around rather freely upon application of a bias voltage, as observed in fully doped PANI (vide infra).

The CITS image and $I-V$ characteristic of fully doped polyaniline (210 nm) film are shown in Figure 7. The conducting inhomogeneity was also observed at applied bias voltage of 0.01 V. However, all $I-V$ curves in various conducting regions showed an ohmic response and the current saturated at the bias voltage less than 0.25 V. Furthermore, all $I-V$ curves are rather symmetrical with respect to 0 V, indicating that the signals are not the same as those observed from typical semiconductor−

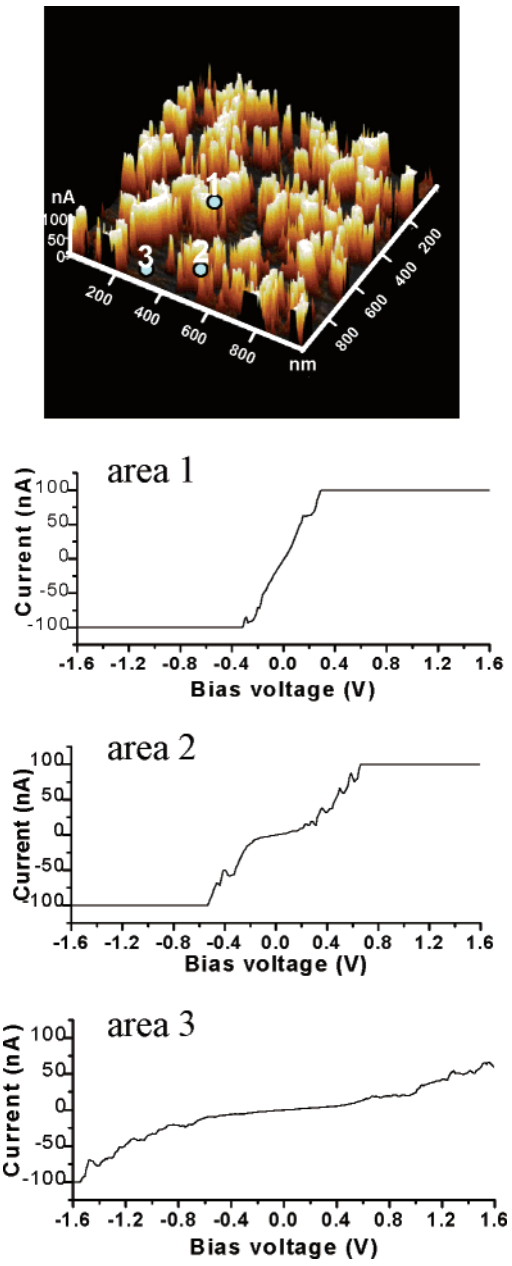

Figure 8. (Upper) CITS image; (lower) $I-V$ curve of fully doped PANI film (160 nm thick, bias voltage 0.5 V).

metal junctions. It was known[17] that conducting polymers become metal-like conductors when heavily doped due to the formation of polaron lattice. The fully doped polyaniline film studied here also showed a metallic conducting behavior, and as expected, the band gap estimated from the $I-V$ curve is ∼0 eV (not shown here). Although the $I-V$ responses for different conducting regions are similar, the conductivity (estimated from the $I-V$ curves) has more than 10 times difference between the highest and the lowest conducting regions. The conductivity of the highest conductive region calculated from eq 2 is 0.5 S·cm^{-1}, which is higher than the bulk conductivity measured with a four-probe method. This result suggested that the bulk conductivity of the PANI film will be affect by the polaron−lattice contact resistance since the polaron lattice in PANI film studied here is not continuous.

As disclosed in the previous paragraphs, the morphology, conductivity, and conducting homogeneity of the fully doped polyaniline films are dependent on the film thickness. It seems that a thin film has less smooth surface and lower but more

homogeneous conductivity. In efforts to assess the electric properties of these films more quantitatively depending on the film thickness, we measured the CITS image and $I-V$ curves at some selected spots of fully doped polyaniline thin (160 nm) film. The results are shown in Figure 8. As can be seen, the conducting homogeneity of thin film is not as good as for a thick film. The $I-V$ curve of the higher conductive region (curve 1) has an ohmic response, limited by the current-limiting of the instrument. On the other hand, the $I-V$ curve in the less conductive region (curve 2) displays characteristics intermediate between pure ohmic and semiconductor behavior, and the lowest conductive region (curve 3) reveals a pure semiconducting characteristic. The band gap energies evaluated from the differential conductance exhibit diverse electric properties. It was found that both metallic (curve 1, zero band gap energy) and semiconducting regions (curves 2 and 3, band gap energies 0.3 and 1.1 eV) were observed in a single fully doped PANI film. The result further supported that the electric properties of PANI films were affected by the aggregation and arrangement of the polymer chains as well as the continuity of the polymer film. To ensure metallic conducting behavior, a sufficient amount of polyaniline chains with few structure defects must be amassed in a polymer film.

Conclusions

Ex situ CITS-AFM is an excellent tool for measuring the local conductivity and current−voltage characteristics of conducting polymers by measuring the current flowing through Au-coated tip/polymer/ITO substrates. It can be used to visualize the heterogeneous electric properties of the 100∼300 nm thick PANI film on ITO substrate. The PANI film has an inhomogeneous conductivity even at the fully doped state. Current images of PANI films recorded in air demonstrate that the electric conductivity of the highest conducting regions of fully doped film is at least 100 times higher than that of the lowest conducting regions. The large spatial variations in the film conductivity on topographically featureless regions were tentatively attributed to the presence of nanoscale crystallites of polaron lattice. This is consistent with the earlier reports, in which conducting islands were observed in doped polyaniline films. The $I-V$ curves of EB film indicated a semiconducing behavior with very high activating energy. The band gap energy of EB film estimated from the derivative conductance is close to those measured from λ_{max} of the UV/vis spectrum and theoretic calculation. Wide-range distribution of band gap energies was found in partially and fully doped PANI films.

Acknowledgment. Financial assistance for this research was provided by the National Science Council, Republic of China (Grant NSC 92-2113-M-008-007).

References and Notes

(1) (a) Singh, R.; Lodha, A. *IEEE Trans. Semicond. Mater.* **2001**, *14*, 281. (b) Saxena, V.; Malhotra, B. D. *Curr. Appl. Phys.* **2003**, *3*, 293. (c) Samuel, I. D. W. *Philos. Trans. R. Soc. London, Ser. A* **2000**, *358*, 193. (d) He, H.; Zhu, J.; Tao, N. J.; Nagahara, L. A.; Amlani, I.; Tsui, R. *J. Am. Chem. Soc.* **2001**, *123*, 7730. (e) Service, R. F. *Science* **2001**, *293*, 782. (f) Skotheim, T. A.; Elsenbaumer, R. L.; Reynolds, J. R. *Handbook of Conducting Polymers*; Marcel Dekker: New York, 1997; Vols. 1−2. (g) Nalwa, H. S. *Handbook of Organic Conductive Molecules and Polymers*; Wiley: Chichester, U.K., 1997; Vols. 1−4. (h) Park, S.-M. In *Handbook of Organic Conductive Molecules and Polymers*; Wiley: Chichester, U.K., 1997; Vol. 3.

(2) (a) Fan, F.-R. F.; Yang, J.; Dirk, S. M.; Price, D. W.; Kosynkin, D. V.; Tour, J. M.; Bard, A. J. *J. Am. Chem. Soc.* **2001**, *123*, 2454. (b) Fan, F.-R. F.; Yang, J.; Cai, L.; Price, D. W.; Dirk, S. M.; Kosynkin, D. V.; Yao, Y.; Rawlett, A. M.; Tour, J. M.; Bard, A. J. *J. Am. Chem. Soc.* **2002**, *124*, 5550. (c) Weiss, P. S.; Bumm, L. A.; Dunbar, T. D.; Burgin, T. P.; Tour, J. M.; Allara, D. L. *Ann. N.Y. Acad. Sci.* **1998**, *852*, 145.

(3) (a) Semenikhin, O. A.; Jiang, L.; Iyoda, T.; Hashimoto, K.; Fujishima, A. *J. Phys. Chem.* **1996**, *100*, 18603. (b) Semenikhin, O. A.; Jiang, L.; Iyoda, T.; Hashimoto, K.; Fujishima, A. *Electrochim. Acta* **1997**, *42*, 3321. (c) Barisci, J. N.; Stella, R.; Spinks, G. M.; Wallace, G. G. *Electrochim. Acta* **2000**, *46*, 519.

(4) (a) Kelley, T. W.; Granstrom, E. L.; Frisbie, C. D. *Adv. Mater.* **1999**, *11*, 261. (b) Gardner, C. E.; Macpherson, J. V. *Anal. Chem.* **2002**, *74*, 576A.

(5) (a) Liau, Y.-H.; Scherer, N. F.; Rhodes, K. *J. Phys. Chem. B* **2001**, *105*, 3282. (b) Planes, J.; Houze, F.; Chretien, P.; Schneegans, O. *Appl. Phys. Lett.* **2001**, *79*, 2993. (c) Gadenne, M.; Schneegans, O.; Houze, F.; Chretien, P.; Desmarest, C.; Sztern, J.; Gadenne, P. *Physica B* **2000**, *279*, 94. (d) Macpherson, J. V.; de Mussy, J. P. G.; Delplancke, J. L. *J. Electrochem. Soc.* **2002**, *149*, B306.

(6) (a) Pouget, J. P.; Jozefowica, M. E.; Epstein, A. J.; Tang, X.; MacDiarmid, A. G. *Macromolecules* **1991**, *24*, 779. (b) Epstein, A. J.; Ginder, J. M. *Synth. Met.* **1987**, *18*, 303. (c) MacDiarmid, A. G.; Epstein, A. J. *Synth. Met.* **1989**, *29*, E409. (d) Lux, F.; Hinrichsen, G.; Krinichnyi, V. I.; Nazarova, I. B.; Cheremisow, S. D.; Pohl, M. M. *Synth. Met.* **1993**, *55*−*57*, 347. (e) Epstein, A. J.; MacDiarmid, A. G.; Pouget, J. P. *Phys. Rev. Lett.* **1990**, *65*, 664. (f) Ginder, J. M.; Richer, A. F.; MacDiarmid, A. G.; Epstein, A. J. *Solid State Commun.* **1987**, *61*, 97. (g) Epstein, A. J.; Ginder, J. M.; Zuo, R. W.; Bigelow, H. S.; Woo, D. B.; Tanner, A. F.; Richer, A. F.; Huang, W.; MacDiarmid, A. G. *Synth. Met.* **1987**, *18*, 303.

(7) (a) Basame, S. B.; White, H. S. *J. Phys. Chem.* **1995**, *99*, 16430. (b) Basame, S. B.; White, H. S. *J. Phys. Chem. B* **1998**, *102*, 9812. (c) Boxley, C. J.; White, H. S.; Gardner, C. E.; Macpherson, J. V. *J. Phys. Chem. B* **2003**, *107*, 9677.

(8) Wu, C.-G.; Hsiao, H.-T.; Yen, Y. R. *J. Mater. Chem.* **2001**, *11*, 2287.

(9) Wu, C.-G.; Chen, P.-Y.; Chang, S.-S. The nanoscale-conducting islands of polyaniline film observed directly from Atomic Force Microscopy-Current Imaging Tunneling Spectroscopy. *Polymer* (submitted for publication).

(10) (a) Leatherman, G.; Durantini, E. N.; Gust, D.; Moore, T. A.; Moore, A. L.; Stone, S.; Zhou, Z.; Rez, P.; Liu, Y. Z.; Lindsay, S. M. *J. Phys. Chem. B* **1999**, *103*, 4006. (b) Sakaguchi, H.; Hirai, A.; Iwata, F.; Sasaki, A.; Nagamura, T.; Kawata, E.; Nakabayashi, S. *Appl. Phys. Lett.* **2001**, *79*, 3708.

(11) Lee, H. J.; Park, S.-M. *J. Phys. Chem. B* **2004**, *108*, 1590.

(12) (a) Yang, R.; Evans, D. F.; Christensen, L.; Hendrickson, W. A. *J. Phys. Chem.* **1990**, *94*, 6117. (b) Yang, R.; Naoi, K.; Evans, D. F.; Smyrl, W. H.; Hendrickson, W. A. *Langmuir* **1991**, *7*, 556.

(13) Ouyang, M.; Huang, J.-L.; Lieber, C. M. *Annu. Rev. Phys. Chem.* **2002**, *53*, 201.

(14) Boudreaux, D. S.; Chance, R. R.; Wolf, J. F.; Schacklette, L. W.; Bredas, J. L.; Themans, B.; Andre, J. M.; Silby, R. *J. Chem. Phys.* **1986**, *85*, 4584.

(15) Park, W. I.; Yi, G.-C.; Kim, J.-W.; Park, S.-M. *Appl. Phys. Lett.* **2003**, *82*, 4358.

(16) (a) Hoier, S. N.; Park, S.-M. *J. Phys. Chem.* **1992**, *96*, 5188. (b) Lee, H. J.; Cui, S.-Y.; Park, S.-M. *J. Electrochem. Soc.* **2001**, *148*, D139. (c) Bredas, J. L.; Themans, B.; Fripiat, J. G.; Andre, J. M. *Phys. Rev. B* **1984**, *29*, 6761.

(17) (a) Sariciftci, N. S.; Heeger, A. J.; Cao, Y. *Phys. Rev. B* **1994**, *49*, 5988. (b) Stafstrom, S.; Bredas, J. L.; MacDiarmid, A. G. *Phys. Rev. Lett.* **1987**, *59*, 1464.